Chemical Engineering Journal 157 (2010) 168–173

Contents lists available at ScienceDirect

Chemical Engineering Journal

journal homepage: www.elsevier.com/locate/cej

A new impinging stream–rotating packed bed reactor for improvement of micromixing iodide and iodate

Weizhou Jiao, Youzhi Liu*, Guisheng Qi

Research Center of Shanxi Province for High Gravity Chemical Engineering and Technology, North University of China, Taiyuan 030051, People's Republic of China

ARTICLE INFO

Article history:
Received 8 September 2009
Received in revised form
22 November 2009
Accepted 24 November 2009

Keywords:
Impinging stream
Rotating packed bed
Micromixing
Segregation index
Iodide–iodate reaction system

ABSTRACT

A novel concept of a liquid–liquid contact reactor, the so-called impinging stream–rotating packed bed (IS–RPB), was presented for improvement of micromixing iodide and iodate. The micromixing efficiency of IS–RPB was studied by adopting iodide–iodate reaction system. The effects of operational conditions (e.g. high gravity factor, liquid flow rate, liquid flow ratio and acid concentration) on micromixing efficiency (characterized by segregation index X_s) were investigated. In addition, the effects of different impinging distance and impinging angle on micromixing efficiency were also considered. Besides, IS, RPB and IS–RPB reactors were contrasted with micromixing characteristics in the same experimental conditions. Comparison with other mixing devices, IS–RPB reactor has better micromixing characteristics than other reactors, which has a good application prospect.

1. Introduction

Micromixing (i.e., mixing at the molecular scale) plays an important role on the quality of products in several industrial reactions such as polymerization, crystallization and precipitation [1]. Micromixing efficiency of many reactors have been studied, including microreactor [2], jet reactor [3], tee mixers [4], rotor–stator mixers [5,6], aerated stirred tank [7], couette flow reactor [8,9], semi-batch reactor [10], static mixer [11], sliding-surface mixing device [12] and so on. Among these reactors, impinging stream (IS) and rotating packed bed (RPB), as the apparatuses of process intensification, have excellent micromixing and mass-transfer efficiency [13,14].

Elperin [15] highlighted firstly IS reactor for intensifying solid–solid and gas–solid mass-transfer efficiency. Becker [16] reported that the concentration distribution of the liquid with laminar flow in the IS reactor. Compared with the bad mixing effect at the fringe of the impinging surface region, the central region of IS have a good micromixing. Moreover, the IS could realize interphase mixing and mass transfer, but it is not mixed or transferred enough for the boundary effect.

Ramshaw [17] invented RPB, a novel gas–liquid reactor that utilized centrifugal acceleration to intensify mixing and mass transfer process. So far, the RPB has been applied to processes widely such as absorption [18–21], distillation [22], micromixing [23], flue gas desulfurization [24] and synthesis of nanoparticles [25–27]. However, the first visual evidence of liquid no uniform distributions was presented by Burns and Ramshaw [28] in a RPB with reticulated PVC packing. The experiment indicated that liquid had the little ability to wander laterally through the packing in comparison with its radial motion. Therefore, the initial liquid distribution will play an important role on micromixing and mass transfer characteristics.

As mentioned above, it enlightened us to design another novel reactor, named impinging stream–rotating packed bed (IS–RPB), according to the intensifying mass transfer and micromixing characteristics. Applying the uniformity of mixing and transfer characteristics of the RPB, the impinging stream and rotating packed bed are combined skillfully in the IS–RPB, which make the liquid/liquid realize better micromixing and mass transfer with higher disperse and turbulent. The high gravity technology is expanded from the gas/liquid to liquid/liquid fields with higher dispersion and turbulence, which has been applied to extraction, liquid membrane separation, emulsion and reaction [29].

The principle of IS–RPB is to bring the two streams flowing along the same axis in the opposite direction into collision to change the liquid non-uniform distribution of RPB, and its impinging spray surface enters the inner brim of RPB along the radial direction. As the result of such a collision, the worse impinging spray surface is farther mixed by the aid of RPB. The predominant mixing characteristics of IS–RPB reactor is that the end effect in the inner radius of RPB offsets the fringe effect of IS, which make the fluid micromixed secondly. Therefore, the coupling between the inner diameter size of RPB and the magnitude of the impinging spray surface plays an important role on avoiding the brim effect of IS and

* Corresponding author. Tel.: +86 351 3921986; fax: +86 351 3921497.
E-mail address: liuyz@nuc.edu.cn (Y. Liu).

1385-8947/$ – see front matter © 2009 Elsevier B.V. All rights reserved.
doi:10.1016/j.cej.2009.11.032

Nomenclature

C_{H^+}	initial concentration of H^+ ion, mol L^{-1}
d	impinging distance, m
g	acceleration of gravity, 9.8 m s^{-2}
K_B	equilibrium constant, L mol^{-1}
L	liquid flow rate, L $h^{-}1$
r_1	inner diameter of IS–RPB, m
r_2	outer diameter of IS–RPB, m
T	temperature, K
V_A	liquid flow rate of A solution, L h^{-1}
V_B	liquid flow rate of B solution, L h^{-1}
X_s	segregation index, dimensionless
Y	selectivity of iodide, dimensionless
Y_{ST}	selectivity of iodide in the case of total segregation, dimensionless

Greek symbols

α	impinging angle,°
β	high gravity factor, dimensionless
η	$\eta = V_A/V_B$ liquid flow ratio, dimensionless

improving the micromixing effect. In present work, the basic structure and characteristics of IS–RPB reactor were introduced firstly, and then the effects of operational conditions and different structures on micromixing efficiency were investigated by employing iodide–iodate reaction system.

2. Experiments

2.1. Basic structure and characteristic of IS–RPB reactor

The main structure of IS–RPB reactor is shown in Fig. 1. The two stainless capillary nozzles were located at the each side of the chamber with an inner diameter of 1 mm. The two different liquid flow along the same axis in the opposite direction into collision. As the result of such a collision, a relatively narrow zone, called the impingement zone of high turbulence intensity, is created which offers excellent conditions for intensifying micromixing and mass-transfer efficiency. Secondly, the collided liquids are redistributed through the rotating packing, which is fully dispersed and flows through the rotor under an imposed collision. Finally, the liquid expelled from the bottom of the IS–RPB.

2.2. Parallel competing reaction system

The mixing at molecular scale is studied by means of competing reactions, these reactions are of two main stoichiometric types: reactive systems such as consecutive competing reactions A + B → R, R + B → S, and parallel competing reactions A + B → R and C + B → S which have the advantage of keeping the memory of mixing efficiency by virtue of the distribution of products. During parallel chemical reactions, which are carried out in a continuous IS–RPB reactor. In 1996, Fournier et al. [30,31] proposed the parallel competing reaction strategy that the $H_2BO_3^-$, I^- and IO_3^- on one hand and H^+ (which is limited reagent) on the other hand are fed separately into the continuous IS–RPB reactor. Its experimental procedure and reactions kinetics were also presented [32,33]. This reaction scheme consists of the following three chemical reactions:

$$H_2BO_3^- + H^+ \leftrightarrow H_3BO_3 \,(\text{quasi-instantaneous}) \quad (1)$$

$$5I^- + IO_3^- + 6H^+ \leftrightarrow 3I_2 + 3H_2O \,(\text{fast}) \quad (2)$$

$$I^- + I_2 \leftrightarrow I_3^- \quad (3)$$

Since the first reaction can be taken as instantaneous, all hydrogen ions are supposed to react with excess $H_2BO_3^-$ with the perfect mixing. Otherwise, iodine will be generated and further reacts with I^- to form I_3^-, as shown in reaction Eq. (3). When the mixing is much faster than Eq. (2), the acid will be almost totally consumed in Eq. (1). However, when the micromixing is slower than Eq. (2) or has the similar rate to Eq. (2), iodine is formed and its yield is a measure of segregation on the molecular scale and incomplete micromixing. The amount of I_3^- produced depends on the micromixing efficiency, and can be detected via the spectrophotometer at 353 nm (Unic Company, USA). The selectivity Y of H^+ and the segregation index X_s were defined respectively.

$$Y = \frac{2\left(n_{I_2} + n_{I_3^-}\right)}{n_{H_0^+}} \quad (4)$$

$$X_s = \frac{Y}{Y_{ST}} \quad (5)$$

$$Y_{ST} = \frac{6C_{IO_{3,0}^-}}{6C_{IO_{3,0}^-} + C_{H_2BO_{3,0}^-}} \quad (6)$$

where Y is the ratio of acid mole number consumed by Eq. (2) divided by the total acid mole number injected and Y_{ST} is the value of Y in total segregation case when micromixing process is infinitely

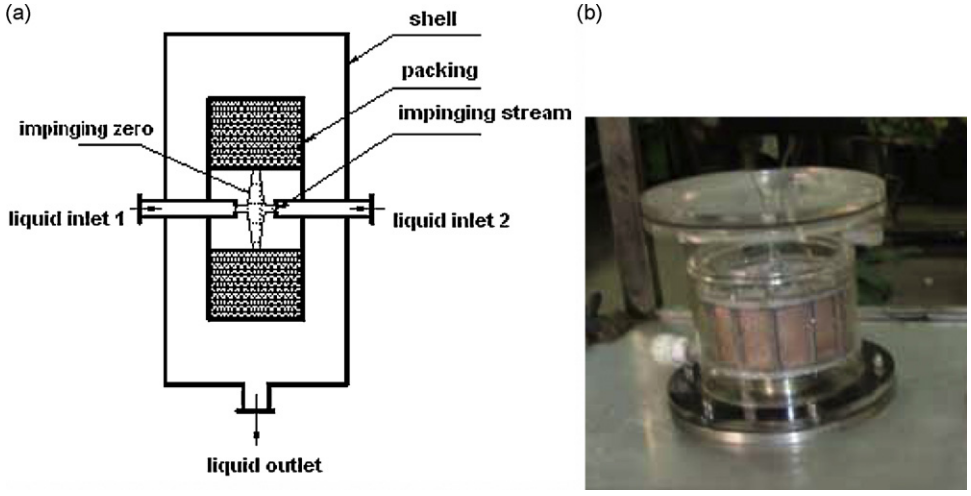

Fig. 1. Schematic of the impinging stream–rotating packed bed unit. (a) Schematic diagram of the IS–RPB; (b) digital photo of the IS–RPB.

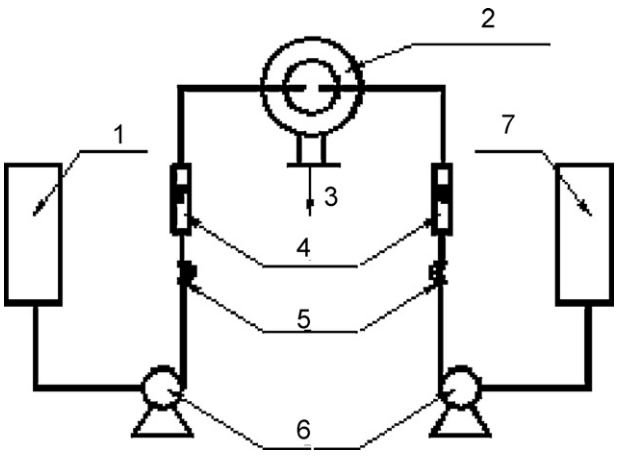

Fig. 2. Schematic diagram of the experimental setup. 1: Stirred tank A; 2: IS–RPB; 3: liquid outlet; 4: rotameter; 5: valve; 6: pump; 7: stirred tank B.

slow. The value of X_s is within the range of $0 < X_s < 1$ for partial segregation, and $X_s = 0$ and $X_s = 1$ indicate the perfect micromixing and the total segregation, respectively. Detailed discussion and calculation of this segregation index X_s can be found in the literature [30].

The mass balances on iodine atoms are showed as the following expression:

$$[I^-] = [I^-]_o - \frac{5}{3}([I_2] + [I_3^-]) - [I_3^-] \quad (7)$$

$$K_B = \frac{[I_3^-]}{[I_2][I^-]} \quad (8)$$

where K_B is the equilibrium constant of Eq. (3), which is the function of temperature T.

$$K_B = \frac{555}{T} + 7.355 - 2.575 \log T \quad (9)$$

By combining these equations, a algebraic equation of iodine concentration are obtained as follows.

$$-\frac{5}{3}([I_2]^2 + ([I^-]_o - \frac{8}{3}[I_3^-])[I_2] - \frac{[I_3^-]}{K_B} = 0 \quad (10)$$

2.3. Experimental section

The main structure of the IS–RPB is shown in Fig. 1. Two liquid streams enter the IS–RPB from different distributors. In our experiments, solutions A and B were prepared firstly. The solution A contains $H_2BO_3^-$, I^- and IO_3^-, while the solution B contains H^+. The packing used in this study is stainless steel wire meshes of 0.3 mm diameter, of 0.96 porosity. The axial height of the bed was 3 cm. The inner and outer radii of the packing were 3 cm and 5 cm, respectively. The rotating speed varied from 500 to 2900 rpm, providing the centrifugal acceleration ranged from 26.5 to 370.2 m/s^2.

Fig. 2 shows the diagram of the experimental setup. The reactants were prepared in two solutions. For the solution A, the boric acid and sodium hydroxide were first added into water, whereafter the potassium iodate and the potassium iodide were introduced into the solution, which ensured the iodide and iodates ions to coexist in a basic solution and prevented iodine from forming. The pH of solutions A was maintained at 9.2 throughout this study. The initial concentration of $H_2BO_3^-$ was 0.09 mol L^{-1}, while for I^-, 1.2×10^{-2} mol L^{-1}, and for IO_3^-, 2.3×10^{-3} mol L^{-1}. The other solution B was H_2SO_4 solution (0.05–0.08 mol L^{-1}, the corresponding H^+ concentration was 0.10–0.16 mol L^{-1}). The flow rate ratio of stream A to stream B was kept at 7. The solution A and B were pumped simultaneously into the IS–RPB after conforming the valves 5 opened and mixed with each other in the bed. If micromixing is homogeneous, then almost all of the injected H^+ reacts with $H_2BO_3^-$ to form H_3BO_3. So reactions (2) and (3) may not occur. Otherwise, the three reactions may all occur. The flowrates of solutions A and B varied from 6 to 140 L h^{-1}. The temperature of solutions were controlled within the range of 19–22 °C. The concentration of I_3^- in the outlet stream was measured by a spectrophotometer at 353 nm.

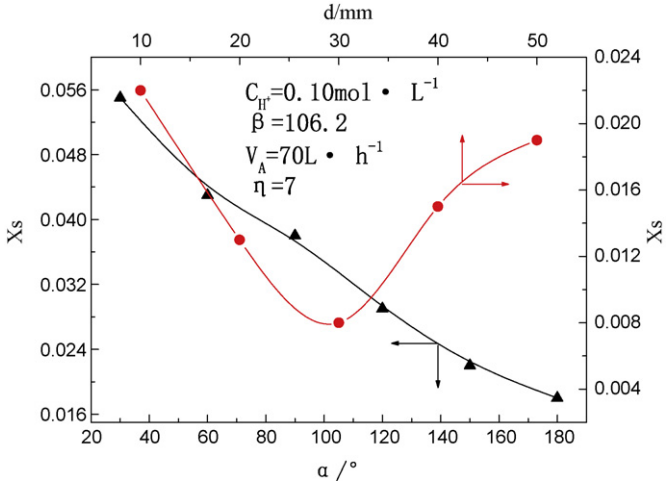

Fig. 3. Influence of the impinging angle α and the impinging distance d on segregation index X_s.

3. Results and discussion

3.1. Effect of the impinging angle α and the impinging distance d on segregation index X_s

The impinging angle α is described as the angle between the two impinging streams. Fig. 3 presented the various of the segregation index X_s with the impinging angle varied from 0° to 180°. It indicated that the segregation index decreased with the augment of impinging angle. For the impinging angle, the direction of the stream through the impinging can affect the efficiency of the micromixing as the impinging angle is changed from acute angle to straight angle. Also, the most effective impinging was produced as the impinging angle was 180°, where the segregation index is 0.018. Therefore, the good micromixing efficiency could be obtained.

The effect of the impinging distances d varied from 10 to 50 mm of IS–RPB on the segregation index X_s was investigated (see Fig. 3). It is clearly seen that the segregation index is dependent on the impinging distance. At the smaller impinging distance, impingement of the jet flows with the very high kinetic energy leads to the pronounced change of the dynamics of the pressure variation in the fluid and is very likely to disturb the coupling between the inner diameter size of RPB and magnitude of impinging spray surface, which the fluid velocity decreases fastly from the tips of nozzles. If the impinging distance is very large, the impingement cannot cause any significant influence on micromixing efficiency and the segregation index would be similar to those obtained by using smaller impinging distance [34]. As shown in Fig. 3, 30 mm is the optimal impinging distance under the condition studied, where the segregation index is 0.008.

3.2. Effect of the high gravity factor β and the acid concentrations C_{H^+} on the segregation index X_s

The high gravity factor β is a ratio of the average high gravitational acceleration in the IS–RPB to the gravitational acceleration.

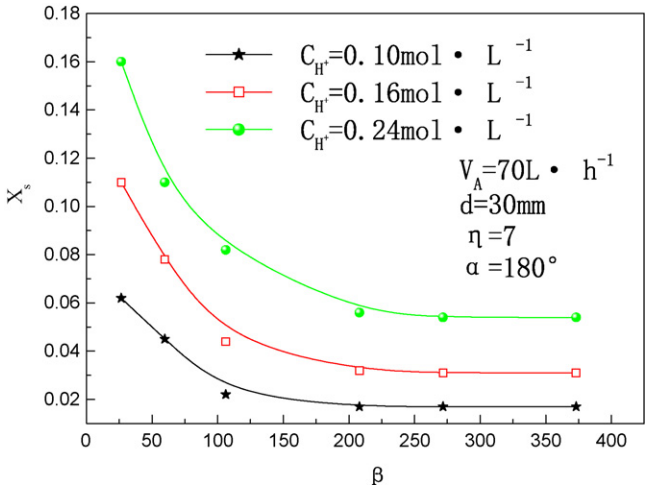

Fig. 4. Influence of high gravity factor β on segregation index X_s under the different acid concentrations.

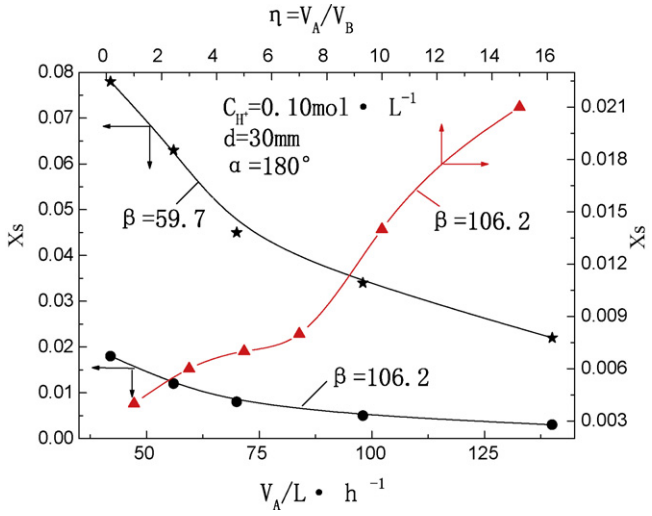

Fig. 5. Influence of the liquid flow rate L and liquid flow ratio η on the segregation index X_s.

Based on the formula (11), the high gravity factor is changed by adjusting the rotor speed or the radius, that is to say, the high gravity fields are changed freely.

$$\beta = \frac{\omega^2 r}{g} \tag{11}$$

Generally, the average high gravity factor describes the magnitude of the high gravity fields ranged from the inner radius to outer radius. In fact, the high gravity field has the characteristics of the cubic distribution, but which is seen as a plane distribution when the packing is axially well-distributed. Therefore, the mean high gravity factor $\bar{\beta}$ is described as the formula (12). Conveniently, the mean high gravity factor $\bar{\beta}$ is replaced by the high gravity factor β.

$$\overline{\beta} = \frac{\int_{r_1}^{r_2} \beta \cdot 2\pi r dr}{\int_{r_1}^{r_2} 2\pi r dr} = \frac{2\omega^2(r_1^2 + r_1 r_2 + r_2^2)}{3(r_1 + r_2)g} \tag{12}$$

Fig. 4 showed the dependence of the segregation index X_s on the high gravity factor β at different acid concentration. It was seen that the segregation index X_s was reduced with the increase of the high gravity factor in the range from 26.5 to106.2. This would be due to the fact that the greater relative velocity among all kinds of liquid elements (e.g. droplet, thread, film) and packing are affected by the rotational speed. Consequently, the frequency of the vigorous impingement and coalescence-dispersion of the liquid elements will quicken, which enhance the micromixing efficiency (smaller X_s) of the IS–RPB. However, when the high gravity factor was further increased (>106.2), only a small effect on X_s was observed. This was probably due to the fact that the extent of reduction in mass-transfer resistances at higher rotating speed was compensated for by a reduction of the residence time that was unfavorable to chemical reaction in the IS–RPB. At the same time, Fig. 4 presented the segregation index X_s as a function of the acid concentrations. It could be seen that the segregation index X_s increased sharply when the acid concentration increased from 0.1 to 0.24 mol L^{-1}. If there is a decrease of the acid concentration, the rate of the proton reaction is slowed down. The rate of the reaction (2) is more sensitive to the acid concentration than that of the reaction (1). Therefore, a high acid concentration will mean a higher production of iodine, which lead to a larger X_s.

3.3. Effect of the liquid flow rate L and the flow rate ratio η on the segregation index X_s

As is shown from Fig. 5, the increase of the liquid flow rate leaded to a steeper decrease of X_s values. This phenomenon may be ascribed to the following two reasons. One reason is that higher liquid flow rates provided higher injecting velocity from the liquid distributor. That is to say, increasing liquid flow rate could result in higher impinging velocity between liquid segments. The other reason is that the residence time distribution (RTD) also decreases with the increasing liquid flow rate. As analogous to the effect of the high gravity factor, a shorter RTD will mean an increase in the coalescence-redispersion frequency between liquid elements and the micromixing rate. Integrating the above analysis, X_s decreases steeply with the increase of the liquid flow rate. For the further increasing the flowrate (>75 L/h), X_s decreases slightly with increasing liquid flow rates. This is due to the fact that the volumes of liquid elements are enlarged slightly as increasing of flow rates, which delay the mixing process of liquid elements and reduce the mixing efficiency. Integrating the above effects, X_s decreases slightly with increasing liquid flow rates.

Fig. 5 showed the various of the segregation index X_s with the flow rate ratio η at V_A = 70 L h^{-1}. In the range of η < 7, X_s < 0.008, implying well micromixing, while out of this range the micromixing becomes poor. This is resulted from macromixing status. For completion of the reaction between A and B to yield a small X_s, the stream B has to contact fully with the stream A. Obviously, this will be much easier when η is smaller, while it needs very strong macromixing for B to contact with almost all the fluid elements containing A when η is large, e.g. η = 15. The macromixing was explained as follows. When the ratio of the liquid flow rate is smaller, it is easier to mix the solution A and B, which need shorter time. However, when the ratio of the flow rate is bigger (e.g. η = 15), one piece of solution A will have to contact simultaneously with 15 pieces of solution B to obtain the better effect, which require the longer time and lead to the worse mixing (bigger X_s).

3.4. Comparison with other mixing devices

At the similar experimental conditions, the segregation indexes X_s of three reactors such as impinging stream (IS), rotating packed bed (RPB) and impinging stream–rotating packed bed (IS–RPB) were compared with iodide–iodate test reactions. Fig. 6 illustrated the effects of the liquid flow rate on X_s with different reactors. The

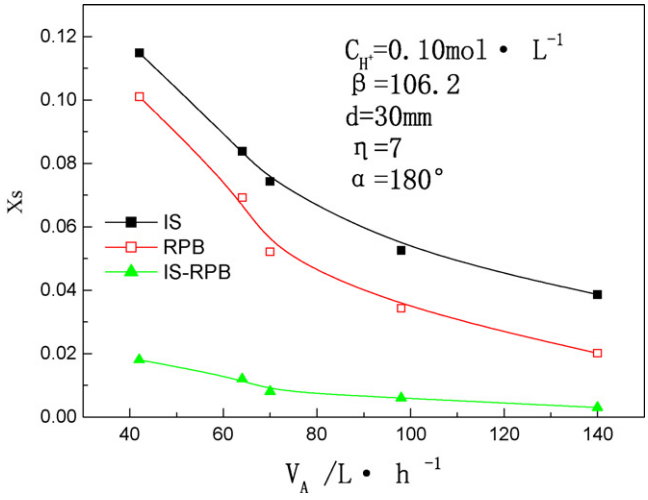

Fig. 6. Influence of the liquid flow rate L on the segregation index X_s with different reactors.

results indicate that a higher liquid flow rate, named a larger liquid injecting velocity, could enhance the micromixing efficiency. Comparison with the three mixing devices, the segregation index X_S of RPB decreased from 0.111 to 0.0201 with the increase of the liquid flow rate. Under the almost same operational conditions, the segregation index X_S of IS–RPB (X_S is less than 0.018) is lower than that of IS reactor and RPB reactor. Meanwhile, compared with other reactors, the segregation index (X_S) of an aerated stirred tank [7] ranged from 0.3 to 0.7. In 1999, Liu et al. [8] measured the micromixing efficiency in a couette flow reactor. They found that X_S decreased from 0.95 to 0.14 with the increase of the rotational speeds. In 2000, Monnier et al. [35] found the micromixing efficiency in a continuous flow cell was enhanced by ultrasound in similar operational condition. They found that the increasing ultrasound power could improve the micromixing efficiency, where X_S varied from 0.03 to 0.07 at the liquid flow rate of 9.53 ml s^{-1}. This indicated that the IS–RPB, with the aid of the centrifugal force and the initial liquid impinging, could improve the micromixing efficiency significantly. Meanwhile, as a continuous mixer or reactor, the large throughout of IS–RPB will further widen its applications in the chemical industry and other industrial domains.

4. Conclusions

Impinging stream–rotating packed bed (IS–RPB) as a novel reactor was introduced according to intensifying mass transfer and micromixing characteristics. Employing iodide–iodate reaction system, the micromixing efficiency of IS–RPB was investigated. In this system, the X_S decreased with the increasing high gravity factor, liquid flow rate and impinging angle. The decrease of the liquid flow ratio results in the decrease of X_S. For the impinging distance, 30 mm is the optimal impinging distance under the operational condition. Comparing the impinging stream (IS) and the rotating packed bed (RPB) devices in the similar operational condition, the micromixing efficiency of IS reactor is the poorest and that of IS–RPB reactor is the best. Comparison with other mixers through the literatures, IS–RPB has a prominent advantage in improving micromixing efficiency, which has a bright prospect for the liquid–liquid mixing.

Acknowledgements

The authors are grateful to the Youth Science and Technology Foundation of Province Shanxi of China and the Graduate Innovation Foundation of Province Shanxi of China for financial support of this work.

References

[1] M. Assirellia, W. Bujalskia, A. Eagleshamb, A.W. Nienowa, Macro- and micromixing studies in an unbaffled vessel agitated by a Rushton turbine, Chem. Eng. Sci. 63 (2008) 35–46.
[2] N. Harries, J.R. Burns, D.A. Barrow, C. Ramshaw, A numerical model for segmented flow in a microreactor, Int. J. Heat Mass Transfer 46 (2003) 3313–3322.
[3] J. Baldyga, J.R. Bourne, R.V. Gholap, The influence of viscosity on mixing in jet reactors, Chem. Eng. Sci. 50 (1995) 1877–1880.
[4] G. Tosun, A study of micromixing in Tee mixers, Ind. Eng. Chem. Res. 6 (1987) 1184–1193.
[5] F. Barailler, M. Heniche, P.A. Tanguy, CFD analysis of a rotor–stator mixer with viscous fluids, Chem. Eng. Sci. 61 (2006) 2888–2894.
[6] J.R. Bourne, M. Studer, Fast reactions in rotor–stator mixers of different size, Chem. Eng. Process. 5 (1992) 285–296.
[7] W.W. Lin, D.J. Lee, Micromixing effects in aerated stirred tank, Chem. Eng. Sci. 21–22 (1997) 3837–3842.
[8] C.I. Liu, D.J. Lee, Micromixing effects in a couette flow reactor, Chem. Eng. Sci. 13–14 (1999) 2883–2888.
[9] J.M. Rousseaux, L. Falk, H. Muhr, E. Plasari, Micromixing efficiency of a novel sliding-surface mixing device, AIChE J. 45 (1999) 2203–2213.
[10] M. Assirellia, W. Bujalskia, A. Eagleshamb, A.W. Nienowa, Intensifying micromixing in a semi-batch reactor using a Rushton turbine, Chem. Eng. Sci. 60 (2005) 2333–2339.
[11] J.Z. Fang, D.J. Lee, Micromixing efficiency in static mixer, Chem. Eng. Sci. 56 (2001) 3797–3802.
[12] B. Judat, A. Racina, M. Kind, Macro- and micromixing in a taylor-couette reactor with axial flow and their influence on the precipitation of barium sulfate, Chem. Eng. Technol. 27 (2004) 287–292.
[13] J.S. Saien, A.E. Zonouzian, A.M. Dehkordi, Investigation of a two impinging-jets contacting device for liquid–liquid extraction processes, Chem. Eng. Sci. 61 (2006) 3942–3950.
[14] J.F. Chen, C. Zheng, G.A. Chen, Interaction of macro- and micro-mixing on particle size distribution in reactive precipitation, Chem. Eng. Sci. 51 (1996) 1957–1966.
[15] I.T. Elperin, Heat and mass transfer in opposing currents, J. Eng. Phys. 6 (1961) 62–68.
[16] H.A. Becker, S.H. Cho, B. Ozum, H. Tsujikawa, Turbulent mixing in the impingement zone of dual opposed free jets and of the normal wall-impinging jet, Chem. Eng. Commun. 67 (1988) 291–313.
[17] C. Ramshaw, Higee distillation—an example of process intensification, Chem. Eng. 389 (1983) 13–14.
[18] D.P. Rao, A. Bhowal, P.S. Goswami, Process intensification in rotating packed beds (HIGEE): an appraisal, Ind. Eng. Chem. Res. 43 (2004) 1150–1162.
[19] K.J. Reddy, A. Gupta, D.P. Rao, Process intensification in a HIGEE with split packing, Ind. Eng. Chem. Res. 45 (2006) 4270–4277.
[20] C.C. Lin, B.C. Chen, Y.S. Chen, S.K. Hsu, Feasibility of a cross-flow rotating packed bed in removing carbon dioxide from gaseous streams, Sep. Purif. Rev. 62 (2008) 507–512.
[21] C.C. Lin, B.C. Chen, Characteristics of cross-flow rotating packed beds, J. Ind. Eng. Chem. 14 (2008) 322–327.
[22] X.P. Li, Y.Z. Liu, Z.Q. Li, X.L. Wang, Continuous distillation experiment with rotating packed bed, Chin. J. Chem. Eng. 16 (2008) 656–662.
[23] H.J. Yang, G.W. Chu, Y. Xiang, J.F. Chen, Characterization of micromixing efficiency in rotating packed beds by chemical methods, Chem. Eng. J. 121 (2006) 147–152.
[24] Y.H. Zhang, L.S. Liu, Y.Z. Liu, Experimental study on flue gas dedusting by high gravity rotary bed, Chin. J. Environ. Eng. 21 (2003) 42–43.
[25] J.F. Chen, Y.H. Wang, F. Guo, X.M. Wang, Synthesis of nanoparticles with novel technology: high-gravity reactive precipitation, Ind. Eng. Chem. Res. 39 (2003) 948–954.
[26] Y. Li, Y.Z. Liu, Synthesis and catalytic activity of copper(II) resorcylic acid nanoparticles, Chem. Res. Chin. Univ. 23 (2007) 217–220.
[27] Y. Li, Y. Guo, Y.Z. Liu, Synthesis of high purity TiO_2 nanoparticles from $Ti(SO_4)_2$ in presence of EDTA as complexing agent, Particuology 3 (2005) 240–242.
[28] J.R. Burns, C. Ramshaw, Process intensification: visual study of liquid maldistribution in rotating packed bed, Chem. Eng. Sci. 51 (1996) 1347–1352.
[29] Y.Z. Liu, Chemical Engineering Process and Technology in High Gravity, National Defense Industry Press, Beijing, 2009, pp. 172–253.
[30] M.C. Fournier, L. Falk, J. Villermaux, A new parallel competing reaction system for assessing micromixing efficiency-experimental approach, Chem. Eng. Sci. 51 (1996) 5053–5064.
[31] M.C. Fournier, L. Falk, J. Villermaux, A new parallel competing reaction system for assessing micromixing efficiency-determination of micromixing time by a simple mixing model, Chem. Eng. Sci. 51 (1996) 5187–5192.
[32] P. Guichardon, L. Falk, Characterisation of micromixing efficiency by the iodide–iodate reaction system. Part I. Experimental procedure, Chem. Eng. Sci. 55 (2000) 4233–4243.

[33] P. Guichardon, L. Falk, J. Villermaux, Characterisation of micromixing efficiency by the iodide–iodate reaction system. Part II. Kinetic study, Chem. Eng. Sci. 55 (2000) 4245–4253.
[34] A. Tsutsumi, M. Ikeda, W. Chen, J. Iwatsuki, A nano-coating process by the rapid expansion of supercritical suspensions in impinging-stream reactors, Powder Technol. 138 (2003) 211–215.
[35] H. Monnier, A.M. Wilhelm, H. Delmas, Effects of ultrasound on micromixing in flow cell, Chem. Eng. Sci. 55 (2000) 4009–4020.